Proton beam divergence measurements from radiation pressure driven shock acceleration

Contact: gc3618@ic.ac.uk

G. Casati, N.P. Dover, O.C. Ettlinger, N. Xu, Z. Najmudin
John Adams Institute for Accelerator Science, Blackett Laboratory, Imperial College London, London, UK

I. Pogorelsky, M. Polyanskiy, W. Li, M. Babzien
Accelerator Test Facility, Brookhaven National Laboratory, Upton, New York 11973, USA

C.A.J. Palmer
School of Maths and Physics, Queen's University Belfast, Belfast, UK

Abstract

Laser-plasma ion acceleration is a fast-developing field of research, yielding ion sources capable of generating high energy, high current, short ion beams. These characteristics make them ideally suited to many applications, including hadron radiation therapy and nuclear physics. We performed a radiation driven, front surface ion acceleration experiment using a long wavelength CO_2 laser to irradiate gas targets. We devised and fielded a proton spatial diagnostic which enabled us to make novel measurements of ion beam divergence. By comparison with shadowgraphy, we observed a relationship between the emission angle of the energetic ions and the electrons generated in the laser plasma interaction. We also observed spatial and spectral modulations of the proton beam on our ion diagnostics.

1 Introduction

In recent years substantial research efforts have been invested in laser driven ion sources. These sources are compact and can deliver high energy (up to 100 MeV[1]), short (ps to ns) ion beams with high peak currents and low emittance. These characteristics make them well suited to many medical, nuclear and material science applications.

There are a number of mechanisms by which high power lasers can accelerate ions [2]. Some mechanisms exploit the ultrahigh radiation pressure of high power lasers to accelerate ions at the front surface of an irradiated opaque target. One such technique is radiation pressure driven collisionless shock acceleration (CSA), in which a target with density just exceeding the plasma critical density n_{crit} is irradiated by a laser pulse with a few ps pulse length. This can generate an electrostatic collisionless shock, which accelerates background ions to to twice the shock velocity [3, 4]. One of the main benefits of CSA is that the produced ion beams can be quasi-mono energetic rather than have a thermal energy spread, which is very attractive for many applications, including radiation therapy [5].

Another desirable characteristic for medical applications is for the beam to contain only one ion species, for example pure helium. This is easily achieved when gas targets are used. However it is difficult to produce gas targets which are over critical to widely used near-infrared high power laser drivers. Equations 1 and 2 show that both the vector potential of the laser, a_0 and the critical density of the plasma, n_{crit}, scale favourably with the laser wavelength λ.

$$a_0 = \frac{eE_0\lambda}{2\pi m_e c^2}, \tag{1}$$

$$n_{crit} = \frac{4\pi^2 m_e \epsilon_0 c^2}{e^2\lambda^2}. \tag{2}$$

These considerations make the long wavelength and high power CO_2 laser at the Accelerator Test Facility at Brookhaven National Laboratory, an ideal choice for exploring radiation pressure acceleration using gaseous targets [6].

Previous studies have shown that collisionless shocks arise in this regime and can accelerate ions in excess of 1 MeV [7, 8]. It was subsequently shown that in order to reliably produce quasi-mono energetic ions it is important for the front surface of the target to have very steep density gradients [9, 10]. This can be achieved by exploiting a laser pre-pulse to shape the target into a spherical blast wave [11].

A technical challenge for many applications of laser driven ion sources is the inherent large beam divergence, which makes it very difficult to couple the ions efficiently to any transport lines. However, the beam divergence in the CSA is not well studied, and previous experiments in these conditions did not measure it.

Therefore, we performed an experiment to study the beam profile of CSA accelerated ions, and investigate its

parametric dependence on gas density. We used the high power CO_2 laser at the Accelerator Test Facility to accelerate protons from a hydrogen gas jet, which could be optically shaped using the pre-pulse. We implemented a tailored scintillator-based beam profile diagnostic accurately measured the proton beams spatial profile. A lower beam divergence was measured when the proton spectrum was quasi-monoenergetic, and a strong dependence on gas pressure was observed.

2 Experimental methods

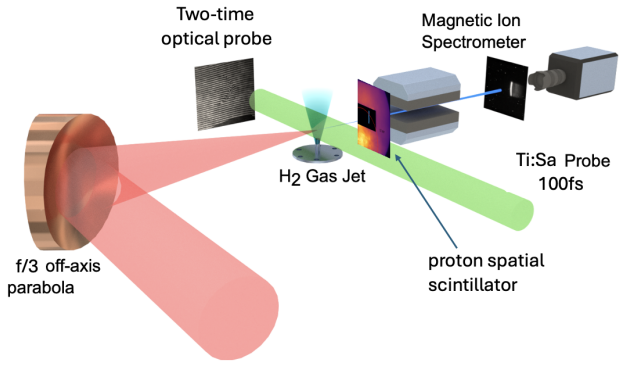

Figure 1: Schematic of our experimental set-up. The red shaded cone represents the CO_2 laser, which is focused by an off-axis parabola onto the hydrogen gas target. The laser-plasma interaction is probed by a 100 fs titanium-sapphire laser, depicted in green in the diagram. Two time interferometry and shadowgraphy are performed using this probe beam. The ions generated in the interaction travel towards the proton spatial diagnostic screen, where a slit allows them to continue their path towards the magnetic spectrometer.

The CO_2 laser used has a wavelength of 9.2 µm, a pulse length of 3 ps, a maximum intensity of $9 \cdot 10^{21}$ W m^{-2} corresponding to $a_0 \approx 5.4$. It delivered 5 J on target and the focal spot size was 25 µm. The hydrogen gas target employed had a flat top density profile. The density was controlled by varying gas pressure. Calibration at a gas pressure of 40 bar showed a density of $5 \cdot 10^{25}$ m^{-3} at 0.65 mm above the nozzle, which is the height of the laser focus. Figure 1 shows the experimental set-up. The CO_2 beam, marked in red, interacts with the target in two steps: first a laser pre-pulse (∼40 mJ) shapes the target into a blast wave, then after a 25 ns delay the main pulse arrives and drives the ion acceleration [9]. An optical probe was implemented using a 100 fs Ti-sapphire laser and it was used to perform two time interferometry and shadowgraphy. To achieve this the probe beam was split in two beams with different polarisations and then added a delay stage to one of the beams' paths to probe the laser-target interaction at a later time. The ion beam produced travels to the proton spatial diagnostic, which uses an EJ-440 scintillator screen shielded by 2.4 µm thick aluminum foil. The screen was sensitive to ion energies above 260 keV. A portion of the ion beam continues its path through a slit in the proton spatial screen, after which it reaches the magnetic spectrometer. This diagnostic uses a magnet to deflect particles based on their momentum, the particles then reach a scintillator screen where their position is directly related to their energy, hence providing the beam's energy spectrum.

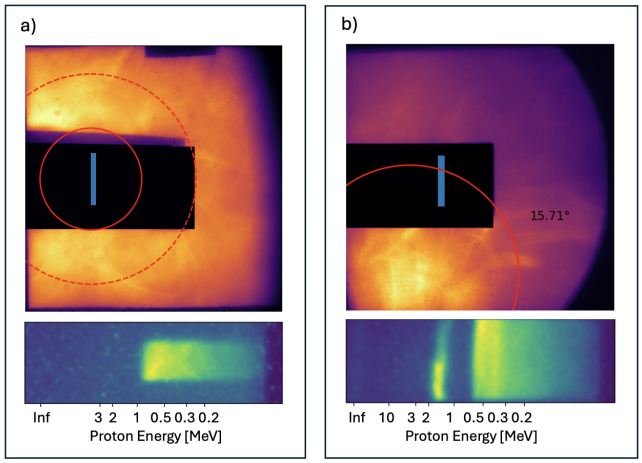

Figure 2: Representative proton spatial (up) and Thompson spectrometer data (below) for two different acceleration modes. The blue region on both scintillator images shows where the Thompson parabola's slit is located spatially. The red circles in a) show the 10° and 20° beam divergence boundaries, in b) the red circle shows the FWHM of the ion beam obtained by fitting Gaussians. Laser energies were 5 J for both shots, the pre-pulse was 5 mJ in a) and 40 mJ in b).

3 Data and results

Figure 2 shows typical examples of the proton spatial profile for a) a low pre-pulse of 5 mJ and b) for 40 mJ. The acceleration mode of the interaction could be controlled by manipulation of the prepulse. With pre-pulses too small to shape the gas jet, thermal beams were always produced. With appropriate prepulse levels of about 40 mJ, quasi-monoergetic features were measured, which is likely to indicate radiation pressure driven collisionless shock acceleration. As highlighted on the figure the divergence of the quasi-monoenergetic ion beam is much lower (15°) than that of the thermal ions ($\gg$20°).

Spatial structure was observed in the quasi-monoenergetic ion beams as shown in figure 2 b). The proton spatial screen displayed significant filamentation of the ion beam while the Thomson spectrometer data shows meaningful spectral variation along the spatial axis.

The vertical position of the proton beams generated

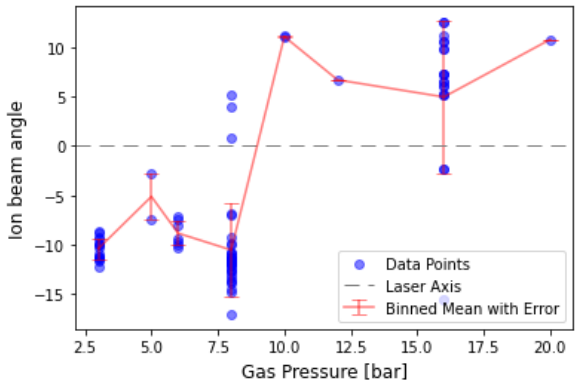

Figure 3: The vertical offset angle of the ion beam centroids for varying gas pressures. The dashed line marks the laser's mean propagation direction. The red line indicates the variation of the centroids' position with pressure.

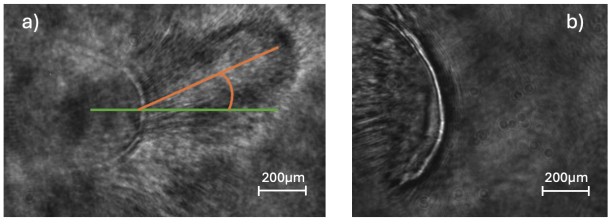

Figure 4: Shadowgraphy of a) a low pressure shot (4 bar) where the electrons' plume was clearly visible and the mean deflection angle is marked, and b) a higher pressure (16 bar) shot where the plasma downstream of the blast wave is homogeneous. The laser and the pre-pulse energies were respectively 8 J and 43 mJ in a) and 7.5 J and 47 mJ in b)

in the collisionless shock acceleration mode was found to vary with gas pressure, as shown in figure 3. At lower pressures, the proton beam pointed below the laser axis, whereas at higher pressures it pointed above.

Figure 4 shows representative shadowgraphy data for a) low and b) high pressure shots, both at $t = 30$ ps after the interaction. Shadowgraphy measurements on low pressure shots indicate a vertical asymmetry in the plasma formation. The prepulse shaped blastwave is clearly visible on the left hand side of both images. The laser propagates from left-to-right, and is absorbed at the blastwave shell. In figure 4 a) a large-scale modulation of the optical probe beyond the blast wave is observed pointing upwards. Shadowgraphy is sensitive to strong changes of gradient in the electron density, and therefore 4 a) indicates the plasma formation is asymmetric in the vertical direction. The plasma formation beyond the blast wave is dominated by field ionisation from the energetic electrons generated by the laser plasma interaction. Hence, the upwards-pointing feature in the shadowgraphy implies that the laser accelerated electrons are also

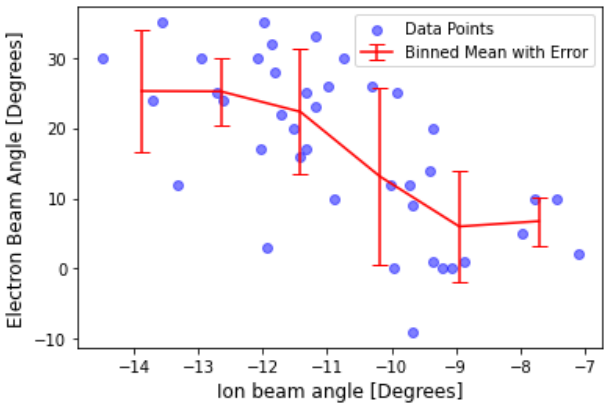

Figure 5: The electrons' deflection angles are plotted versus the corresponding ions' deflection angles. The red line which is a trend of the data after binning shows a general negative trend

propagating in that direction. The ion beams produced in these shots pointed downwards with respect to the laser direction. The fine scale transverse modulation of the plasma is due to a Weibel-like current filamentation instability [12].

Despite the fact that the blastwave is evident for higher gas pressures (Figure 4 b)), the behaviour downstream of the shock is very different; there is no clear asymmetry in this case, but the ions generated seem to point upwards.

Figure 5 takes into account low pressure shots and shows the relationship between the characteristic angle of the plasma formation and the corresponding ion beams' deflection angle. There is a clear negative correlation, suggesting that these two asymmetries are inversely linked, the more the ions point downwards, the more the electrons point upwards.

An explanation for the vertical asymmetry is an offset between the centre of the blast wave and the laser focus. As the blast wave surface is curved, any off-set would result in a change in the effective angle of incidence onto the density gradient. Despite the blast wave shaping, there is still a relatively long density scale length which would cause laser refraction before reaching the critical surface. Therefore, if the laser was focused below the centre of the blast wave, the slight angle of the gas target would cause the laser to refract upwards. The generated electrons are then preferentially accelerated in the shifted laser propagation direction as they follow the laser. On the other hand, the protons will be accelerated along the surface normal direction, which would translate to a downward tilt. The ions' deflection should be more marked the further the laser focus is from the centre of the blast wave, and indeed this appears to be the case in our data as shown by figure 3. Simulations are being performed to further elucidate the observed acceleration dynamics.

4 Conclusions

We performed an experiment where a high intensity ($9{\cdot}10^{21}\mathrm{W\,m^{-2}}$) laser interacted with near critical density plasma and we were able to directly probe the interaction, obtaining sharp shadowgraphy and interferometry data.

We also fielded an innovative proton spatial diagnostic which allowed us to measure the divergence of our ion beams. We compared the divergence of thermal ions produced in a sheath acceleration regime and that of quasi-mono energetic ions and we found that the latter was significantly smaller.

The proton spatial data in conjunction with the shadowgraphy data revealed that both ions and electrons travelled away from the target at an angle with respect to the laser propagation direction. There is a reciprocal relationship between the deflection angles of the electrons and ions which could be explained by assuming that the laser impacts the blast wave target a certain vertical distance away from its centre.

We also observed spatial modulation on both ion diagnostics, further work is needed to understand exactly what the source of these features is.

Being able to identify, explain and eventually tailor the spatial properties of the ion beam distribution is important for all applications. In particular a better understanding of the ion divergence and deflection angles would allow for enhanced coupling between the beams and transport lines.

Acknowledgments

This work was supported by UK STFC grant ST/V001639/1, Vulcan Shutdown Support 24810007, and EUs Horizon 2020 research and innovation program under the Marie Sklodowska-Curie grant agreement No 894679. We would like to thank the technical support team at the Accelerator Test Facility for their support.

References

[1] T. Ziegler et al. Laser-driven high-energy proton beams from cascaded acceleration regimes. *Nat. Phys.* **20,** (2024), pp. 1211–1216.

[2] H. Daido, M. Nishiuchi, and A. S. Pirozhkov. Review of laser-driven ion sources and their applications. *Reports on Progress in Physics* **75,** (2012), p. 056401.

[3] J. Denavit. Absorption of high-intensity subpicosecond lasers on solid density targets. *Phys. Rev. Lett.* **69,** (1992), pp. 3052–3055.

[4] L. O. Silva et al. Proton Shock Acceleration in Laser-Plasma Interactions. *Phys. Rev. Lett.* **92,** (2004), p. 015002.

[5] A. Macchi, M. Borghesi, and M. Passoni. Ion acceleration by superintense laser-plasma interaction. *Rev. Mod. Phys.* **85,** (2013), pp. 751–793.

[6] M. N. Polyanskiy, I. V. Pogorelsky, and V. Yakimenko. Picosecond pulse amplification in isotopic CO2 active medium. *Opt. Express* **19,** (2011), pp. 7717–7725.

[7] C. A. J. Palmer et al. Monoenergetic Proton Beams Accelerated by a Radiation Pressure Driven Shock. *Phys. Rev. Lett.* **106,** (2011), p. 014801.

[8] D. Haberberger et al. Collisionless shocks in laser-produced plasma generate monoenergetic high-energy proton beams. *Nat. Phys.* **8,** (2012), pp. 95–99.

[9] O. Tresca et al. Spectral Modification of Shock Accelerated Ions Using a Hydrodynamically Shaped Gas Target. *Phys. Rev. Lett.* **115,** (2015), p. 094802.

[10] N. P. Dover et al. Optical shaping of gas targets for laser–plasma ion sources. *Journal of Plasma Physics* **82,** (2016), p. 415820101.

[11] L. I. Sedov. *Similarity and Dimensional Methods in Mechanics*. New York: Academic Press Inc., 1959. Chap. 63.

[12] N.P. Dover et al. *Optical imaging of laser-driven fast electron Weibel-like filamentation in over-critical density plasma*. submitted (2024).